International Journal of Recent Engineering Research and Development (IJRERD)
Volume No. 02 – Issue No. 05, ISSN: 2455-8761
www.ijrerd.com, PP. 49-59

Nonlinear Adaptive Control of Parameter Uncertain Unmanned Surface Vehicle Heading

Shahbaz Nawaz, Mateen Ul Haque
COMSATS Institute of IT, Department of Electrical Engineering,
The Mall, Wah 47040, Pakistan

Abstract: An unmanned surface vehicle is a water surface float boat with many practical applications and it also acts as a testbed for simulation and verification of control algorithms. The control of yaw dynamics of an unmanned surface boat using nonlinear adaptive control method has been considered. The system parameters are assumed unknown and the technique of nonlinear adaptation using manifold immersion is performed for their estimation. Reference tracking is obtained. The experimental validation of the theoretically proposed controller is presented by implementing discrete time realization of control algorithm using digital controller interfaced in real time with Simulink. The potential of proposed algorithm relies upon the flexibility in the structure of control algorithm and promising transient behavior of closed loop system dynamics.
Keywords: unmanned surface vehicle, adaptive control, manifold immersion, adaptive parameter estimation.

1. Introduction

An Unmanned Surface Vehicle (USV) or Autonomous Surface Vehicle (ASV) is a marine vehicle that lies in the domain of Remotely Operated Vehicles (ROV) running on water surface. It has various commercial applications as well as military uses. It has no crew so it presents many advantages in military applications and dangerous or tedious environmental conditions by reducing risk of loss of human life and time saving. They can be deployed to perform tasks such as mine counter measures, surveillance and reconnaissance, anti-submarine warfare, fast inshore attack craft, combat training, oil and gas exploration and construction, oceanographic data collection, hydrographic, oceanographic and environmental surveys.

There is a boom in the development of USV over past few decades. The unpredictable environmental conditions and complex dynamics of USVs make them a challenging system to be modelled and controlled. It also acts as a benchmark to simulate and test new and advanced control techniques. A mini USV boat has nonlinear dynamics. Moreover, by involving dynamics of the driving motor-rudder actuator along with the motor amplifier, complicates the problem still more as it adds more state variables in system dynamics, which tantamount to increase in the order of the system. To add to the difficulty, there are various uncertain system parameters. Hence there is always a room for a better and effective control technique for USV boat.

There are various control techniques available in literature. A control system architecture is designed for an unmanned surface vehicle in [1] and the composing and function of the modules of the control system architecture are detailed in this work. A finite-time trajectory tracking control approach is proposed for an unmanned surface vehicle with unknown external disturbances and input saturation in [2]. An adaptive linear parameter varying (LPV) fault tolerant control approach is applied to an unmanned surface vehicle steering control in [3]. An autopilot is designed for an unmanned surface vehicle subject to dynamical uncertainty, time-varying ocean disturbances and unmeasured yaw rate in [4], where output feedback adaptive steering law is developed based on a state observer and a neural network using iterative updating law. System identification tests were conducted to get the precise model of the USV in [5] followed by design of a sliding mode controller and a wind feedforward controller to aid the nonlinear feedback control to mitigate wind disturbance. An adaptive fuzzy logic control scheme with back-stepping for tracking unmanned surface vehicles (USV) in the framework of uncertain strict-feedback nonlinear system with unknown dynamics and external disturbances is proposed in [6]. A survey on control allocation algorithms in tactical level control for path tracking unmanned surface vehicles is conducted in [7]. A finite-time trajectory tracking control problem of an unmanned surface vehicle with external disturbances in considered in [8]. The experimental testing of an unmanned surface vehicle has been performed to evaluate the performance of two low-level controllers, when displacement and drag properties are time varying and uncertain has been performed in [9]. A control methodology of SVM inverse model for unmanned surface vehicle system heading control is presented in [10].

Most of these techniques consider the linear system model or a reduced order model of the system. Moreover, controllers do not have many tunable parameters to gain much control over system responses. Many controllers suffer degradation of response as the operation conditions change or the system parameters vary with time. We have applied a robust adaptive nonlinear control algorithm that relies on robustification of reduced order system controller against full order system dynamics [11]. The controller is also robust against unknow system parameters and has a lot of free tunable parameters to gain control over feedback dynamic response of the system output.

2. Overview of Hardware

The hardware is shown in Figure 1. It consists of a surface float boat. It is powered by a battery with a mission time of about 25 minutes. The body of the boat is propelled by a propeller, which is attached to a thruster motor by a connecting shaft. Heading of the boat is controlled by a rudder. Rudder is actuated by a servo motor. The propeller and rudder are shown in Figure 2.

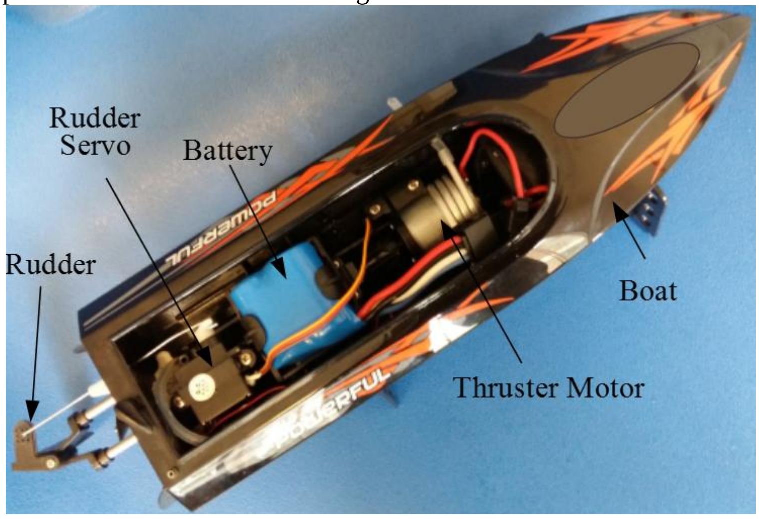

Figure 1: An overview of the hardware

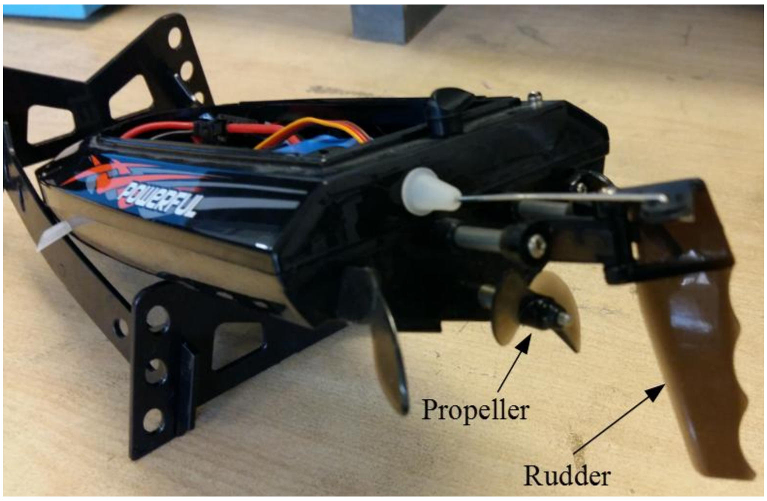

Figure 2: Actuation mechanism in boat.

3. The Control Algorithm Synthesis

Consider a nonlinear parameter uncertain system,

$$\dot{\underline{p}} = \underline{s}\left(\underline{p}, u_e\right) = \underline{f}\left(\underline{p}\right) + \underline{g}\left(\underline{p}\right) u_e \tag{1}$$

where $\underline{p} \in \mathbb{R}^n$ and $u_e \in \mathbb{R}^m$. The state vector $\underline{p}$ evolves on a smooth manifold P of dimension n, which is spanned by tangential manifold to the system map $\underline{s}$. The system map $\underline{s}$ in Equation 1 has been decomposed into a drift vector field $\underline{f}(.)$ and a controlled vector field $\underline{g}$. In Equation 1, $u_e \in U\left(\underline{p}\right)$ is the system forcing function with U a state dependent input set which belongs to the control bundle $\bigcup_{\underline{p} \in \mathrm{P}} U\left(\underline{p}\right)$. The topological manifold immersion based nonlinear control approach involves defining a reduced order exosystem. The state trajectories of the exosystem evolve on a C^{∞} submanifold $\mathrm{Q} \subset \mathrm{P}$. The problem of controller design then boiled down to synthesize a control law that dynamically immerses the state trajectories of full order system to the manifold Q. Let us consider an exosystem with state vector $\underline{q} \in \mathbb{R}^q$ with $q < n$, which contains origin in its reachable set. This can be achieved by defining the vector field $\underline{\Upsilon}(\underline{q})$ of the exosystem that governs the evolution of $\underline{q}$ as given by Equation 2.

$$\dot{\underline{q}} = \underline{\Upsilon}(\underline{q}) \tag{2}$$

Defining a smooth submanifold for the exosystem of Equation 2 as:

$$\mathrm{Q} = \left\{ \underline{p} \in \mathbb{R}^n \middle| \underline{p} = \underline{\psi}(\underline{q}); \underline{q} \in \mathbb{R}^q \right\} \tag{3}$$

The controlled integral curves of system map $\underline{s}$ can be attracted by the submanifold Q if partial differential Equation 4 along with the condition in Equation 5 is satisfied [9].

$$\underline{f}\left(\underline{\psi}(\underline{q})\right) + \underline{g}\left(\underline{\psi}(\underline{q})\right)\wp(\underline{\psi}) = L_{\Upsilon}\underline{\psi} \tag{4}$$

$$\underline{q}(t) = \underline{0} \quad \forall \ \underline{q}(0) \in \mathbb{R}^2 \text{ as t} \to \infty \tag{5}$$

Here $L_{\Upsilon}\underline{\psi} = (\nabla_{\underline{q}}\underline{\psi})\underline{\Upsilon}(\underline{q})$ is the so-called Lie derivative. Also $\wp\left(\underline{\psi}(\underline{q})\right) = v\left(\underline{\psi}(\underline{q}), 0\right)$ on the submanifold Q and $u = v\left(\underline{p}, \zeta(\underline{p})\right)$ is the synthesized feedback control law that renders Q attractive, $\zeta(.)$ is the implicit description of Q and it is given by parameterized form in Equation 6.

$$\zeta(\underline{p}) = \underline{p} - \underline{\psi}(\underline{q}) = 0 \tag{6}$$

Introducing state variable $\hbar$ to define "off" the submanifold Q dynamics given by:

$$\dot{\hbar} = L_{\underline{s}}\zeta\big|_{u=\vartheta(\underline{p},\hbar)} = \left(\frac{\partial\zeta}{\partial\underline{q}}\right)\underline{s}\left(\underline{p}, \vartheta(\underline{p}, \hbar)\right) \tag{7}$$

In terms of $\hbar$ and any constant $\alpha > 0$, the synthesized controller ϑ the system mapping is given by,

$$\dot{\underline{p}} = \underline{s}\left(\underline{p}, \vartheta(\underline{p}, \hbar)\right) \tag{8}$$

For any general system of form,

$$\begin{aligned} \dot{\underline{p}}_1 &= \underline{\xi}_1(p_1) + \underline{\xi}_2(\underline{p}_1)p_2 \\ \dot{p}_2 &= \underline{\varphi}(\underline{p})^T\underline{\lambda}_1 + \lambda_2 u \end{aligned} \tag{9}$$

where $\underline{\xi}_i(.)$ and $\underline{\varphi}(.)$ are smooth mappings, λ_i are unknown parameters and $\dot{\underline{p}}_1 = \underline{\xi}_1(\underline{p}_1)$ is globally stable, then for constants $\varepsilon > 0$ and $k > 0$, the geometric adaptive estimates of λ_i are given by [9].

$$\dot{\hat{\underline{\lambda}}} = -\left(I + \nabla_{\hat{\underline{\lambda}}}\underline{\upsilon}\right)^{-1}\begin{pmatrix} \left(\nabla_{\underline{p}_1}\underline{\upsilon}\right)\left(\underline{\xi}_1(\underline{p}_1) + \underline{\xi}_2(\underline{p}_1)p_2\right) \\ +\dfrac{\partial\underline{\upsilon}}{\partial p_2}\left(-kp_2 - \varepsilon L_{\underline{\xi}_2}V_1(\underline{p}_1)\right) \end{pmatrix} \tag{10}$$

and the corresponding geomantic synthesized control law is given by,

$$u = -\left(\hat{\lambda}_2 + \upsilon_2(\underline{p}, \hat{\underline{\lambda}}_1)\right)\begin{pmatrix} kp_2 + \varepsilon L_{\underline{\xi}_2}V_1(\underline{p}_1) \\ +\varphi(\underline{p})^{\mathrm{T}}\left(\hat{\underline{\lambda}}_1 + \underline{\upsilon}_1(\underline{p})\right) \end{pmatrix} \tag{11}$$

The vector $\underline{\upsilon} = \left[\underline{\upsilon}_1(\underline{p}) \quad \upsilon_2(\underline{p}, \hat{\underline{\lambda}}_1)\right]^{\mathrm{T}}$ is given by:

$$\underline{\upsilon}_1(\underline{p}) = \gamma_1\int_0^{p_2}\varphi(\underline{p}_1, \eta)d\eta \tag{12}$$

$$\begin{aligned} \upsilon_2(\underline{p}, \hat{\underline{\lambda}}_1) = \gamma_2&\left(k\frac{p_2}{2} + \varepsilon L_{\underline{\xi}_2}V_1(\underline{p}_1)p_2\right) \\ &+\gamma_2\int_0^{p_2}\varphi(\underline{p}_1, \eta)^{\mathrm{T}}\left(\hat{\underline{\lambda}}_1 + \underline{\upsilon}_1(\underline{p}_1, \eta)\right)d\eta \end{aligned} \tag{13}$$

According to [10], $V_1(\underline{p}_1)$ is any mapping such that for some class-K function $\kappa(.)$, we have,

$$L_{\underline{\xi}} V_1(\underline{p}_1) \leq -\kappa(\underline{p}_1) \tag{14}$$

and $\gamma_1 > 0$, $\gamma_2 > 0$ are constants.

4. Experimental Testbed and System Dynamics

Consider the experimental testbed of twin rotor mechanism in the Figure 2.

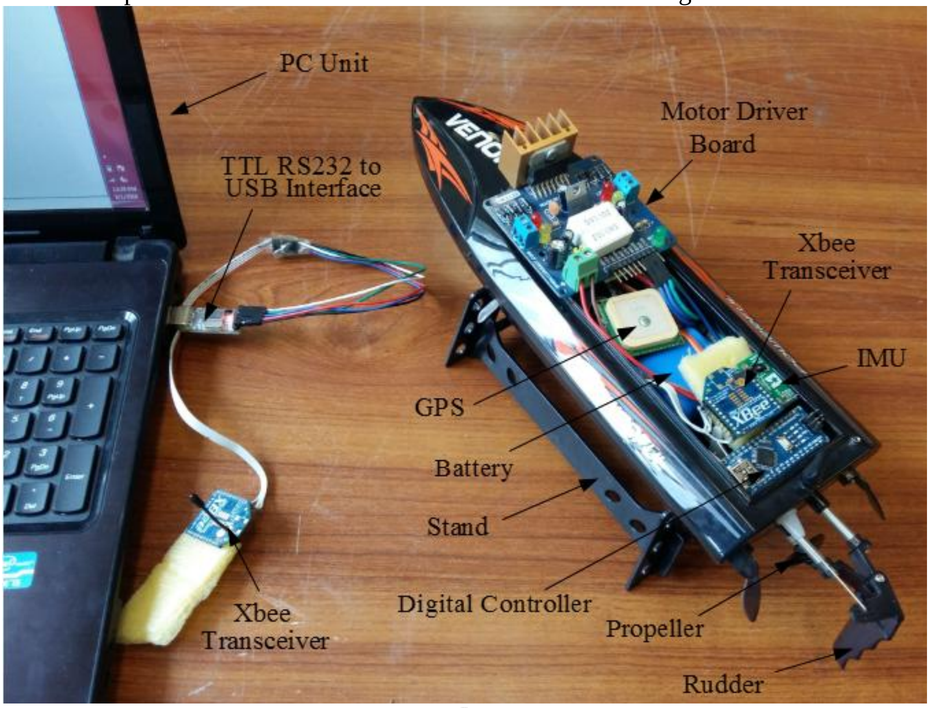

Figure 3: An overview of the experimental setup.

If ψ denotes pitch angle of main rod and δ denotes the angular displacement of rudder then the system state variables for yaw dynamics are described by Equation 15.

$$\underline{p} = \begin{bmatrix} p_1 & p_2 & p_3 \end{bmatrix}^T = \begin{bmatrix} \psi & \dot{\psi} & \delta \end{bmatrix}^T \tag{15}$$

If we consider the first order curve fit for the rudder angle against its driving signal then the dynamics of system are described by following system of Equation 16. Force decomposition is shown in Figure 4.

$$\begin{aligned} \underline{f}\left(\underline{p}\right) &= \begin{bmatrix} p_2 & -k_1 p_2 + k_2 p_3 & -p_3 k_3 \end{bmatrix}^T \\ \underline{g}\left(\underline{p}\right) &= \begin{bmatrix} 0 & 0 & k_4 \end{bmatrix}^T \\ \underline{s}\left(\underline{p}, u_e\right) &= \begin{bmatrix} p_3 & -k_1 p_2 + k_2 p_3 & -p_3 k_3 + k_4 u_e \end{bmatrix}^T \end{aligned} \tag{16}$$

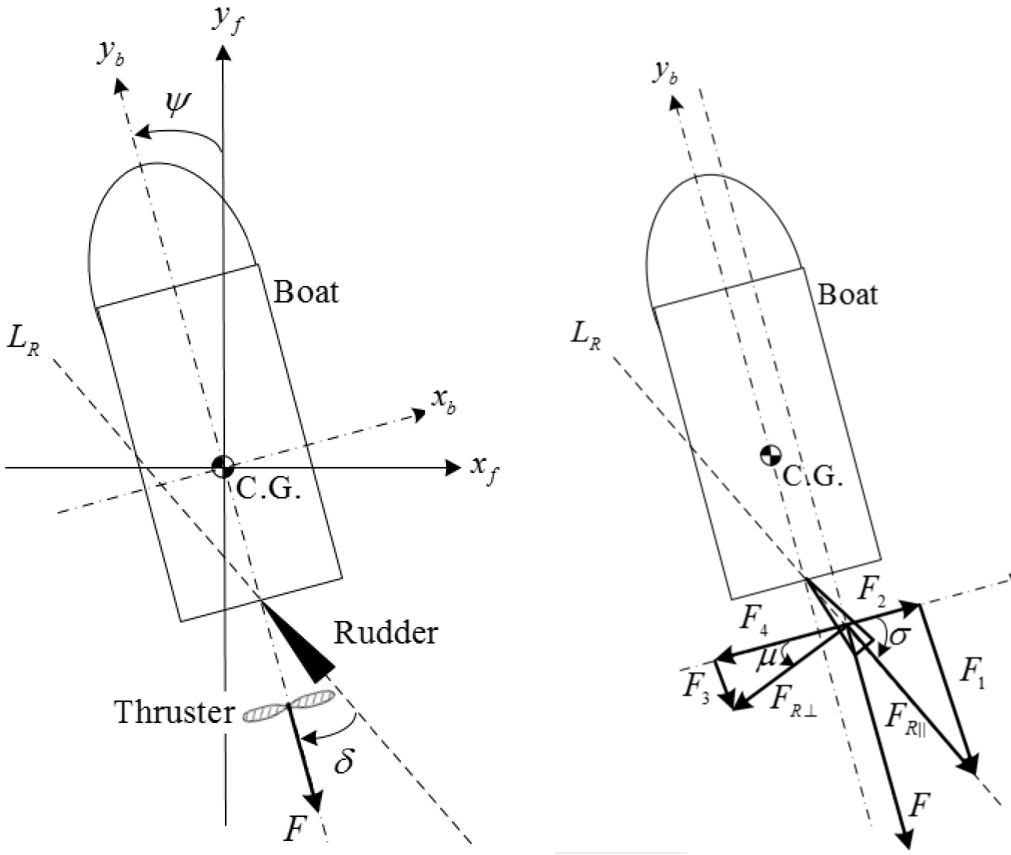

(a) **(b)**

Figure 4: Force vector decompositions

Equation 2 and Equation 8 evaluate to following expressions.

$$\underline{\Upsilon}\left(\underline{q}\right)=\left[q_2 \quad -k_1+k_2\varsigma_1^{\,2}\right]^{T} \tag{17}$$

$$\underline{p}=\underline{\psi}\left(\underline{q}\right)=\left[q_1 \quad q_2 \quad \psi_1\left(q_1,q_2\right)\right]^{T} \tag{18}$$

$$\vartheta\left(\underline{p},\hbar\right)=\frac{-\alpha\hbar+\dot{\varsigma}_1+k_3p_3}{k_4} \tag{19}$$

The reduced order system is given by Equation 20.

$$\begin{aligned}\dot{\hbar}&=-\alpha\hbar\\ \dot{p}_1&=p_2\\ \dot{p}_2&=-k_1p_2+k_2\varsigma_1\\ \dot{p}_3&=-\alpha\hbar+\dot{\varsigma}_1\end{aligned} \tag{20}$$

The system in Equation 20 immerses to system described by Equation 21.

$$\begin{aligned}\dot{p}_1&=p_2\\ \dot{p}_2&=-k_1+k_2\varsigma_1\end{aligned} \tag{21}$$

Renaming the control input of Equation 21 as,

$$\varsigma_1=u \tag{22}$$

The immersion control law is given by,

$$\vartheta\left(\underline{p},\hbar\right)=\frac{-\alpha\hbar+\dot{\varsigma}_1+k_3p_3}{k_4} \tag{23}$$

Using Equation 21 and Equation 22 we get,

$$\dot{\underline{p}} = \begin{bmatrix} p_2 & -k_1 p_2 + k_2 u \end{bmatrix}^{\mathrm{T}} \tag{24}$$

For the estimation of unknown parameters in Equation 24, using the results in Equation 9 through Equation 14, we get.

$$\underline{\xi}_1(p_1) = 0, \quad \underline{\xi}_2(\underline{p}_1) = 1$$

$$\lambda_1 = k_1, \qquad \lambda_2 = k_2 > 0 \tag{25}$$

$$\varphi(\underline{p}) = -1$$

$$L_{\underline{\xi}_2} V_1(\underline{p}_1) = 2\underline{p}_1 \tag{26}$$

$$\underline{\upsilon} = \begin{bmatrix} c_1 p_2 \\ c_2 p_2^2 +_1 c_3 \hat{\lambda}_1 p_2 + c_4 p_1 p_2 \end{bmatrix} \tag{27}$$

$$\nabla_{\hat{\underline{\lambda}}} \underline{\upsilon} = \begin{bmatrix} 0 & 0 \\ -\gamma_2 p_2 & 0 \end{bmatrix} \tag{28}$$

$$\nabla_{\underline{p}_1} \underline{\upsilon} = \frac{\partial \underline{\upsilon}}{\partial p_1} = \begin{bmatrix} 0 & 2\varepsilon\gamma_2 p_2 \end{bmatrix}^{\mathrm{T}} \tag{29}$$

$$\frac{\partial \underline{\upsilon}}{\partial p_2} = \begin{bmatrix} -\gamma_1 & k\gamma_2 p_2 + 2\gamma_2 k p_1 - \gamma_2 \hat{\lambda}_1 + \gamma_1 \gamma_2 p_2 \end{bmatrix}^{\mathrm{T}} \tag{30}$$

The parameter estimates in Equation 10 leads us to,

$$\dot{\hat{\underline{\lambda}}} = \begin{bmatrix} c_5 p_1 + c_6 p_2 \\ c_7 p_1^2 + c_8 p_2^2 + c_9 p_1 p_2 + c_{10} p_2 \hat{\lambda}_1 + c_{11} p_1 \hat{\lambda}_1 \end{bmatrix} \tag{31}$$

The control law in terms of estimates parameters is given by,

$$u = -\left(\hat{\lambda}_2 + \upsilon_2(\underline{p}, \hat{\underline{\lambda}}_1)\right)\left(kp_2 + 2\varepsilon p_1 - \hat{\underline{\lambda}}_1 - \underline{\upsilon}_1(\underline{p})\right) \tag{32}$$

At the last the reference tracking is achieved by modifications of control law as,

$$\vartheta_1\left(\underline{p}, \hbar\right) = \frac{-\alpha\hbar + \dot{\varsigma}_1 + k_3 p_3}{k_4} + \sigma(t) \tag{33}$$

A typical classical proportional derivative tracker law can be used to follow reference command as given by,

$$\sigma(t) = \Xi(e(t)) \tag{34}$$

$$\Xi(.) = -\frac{k_3}{k_4}\left(k_p(.) + k_d \frac{d(.)}{dt}\right) \tag{35}$$

5. Simulation and Experimental Results

The Simulink model of the closed loop system with reference tracker is shown in Figure 5. The actual values of the system parameters in the system modelling equations are given in Table 1.

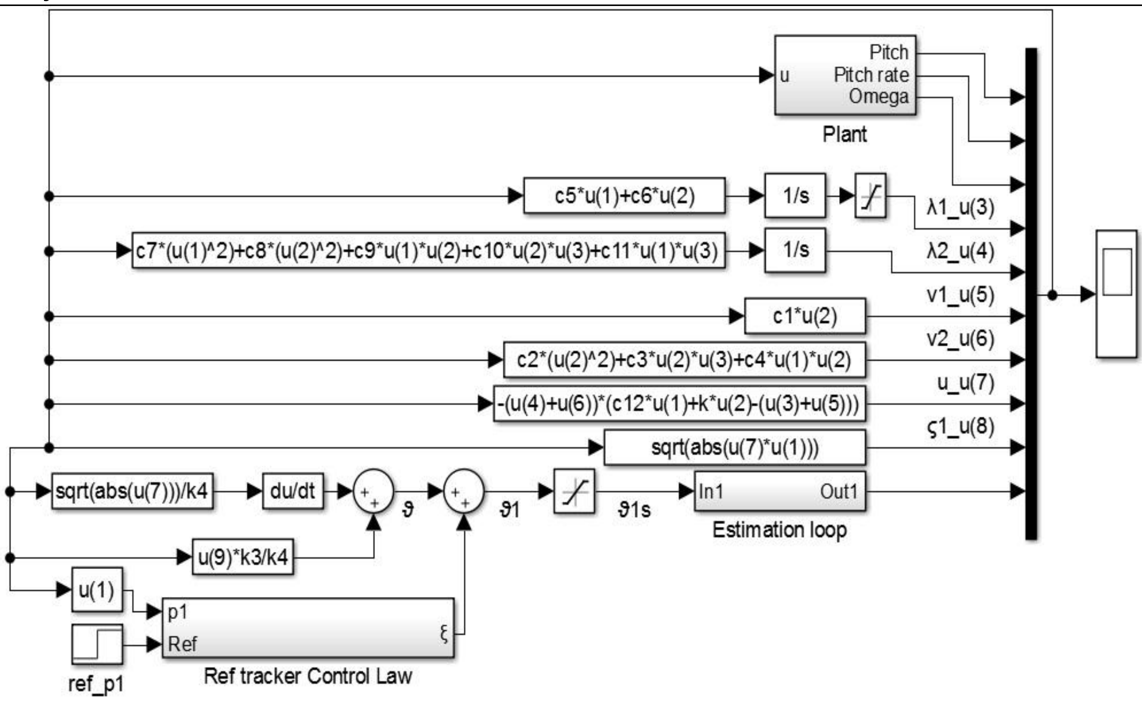

Figure 5: Simulink model of the closed loop system

Table 1: Numerical values of the system parameters.

Parameter	*Value*	*Parameter*	*Value*
k_3	145	c_4	0.018
k_4	7.15	c_5	-0.25
k	61	c_6	-214
γ_1	4.1	c_7	5×10^{-4}
γ_2	1.0	c_8	845.0
ε	2.1×10^{-3}	c_9	0.25
c_1	-6.25	c_{10}	-750.0
c_2	72.0	c_{11}	-0.05
c_3	-3.25	c_{12}	0.125

The simulation result for yaw response is shown in Figure 6. The response is stable with zero steady state error.

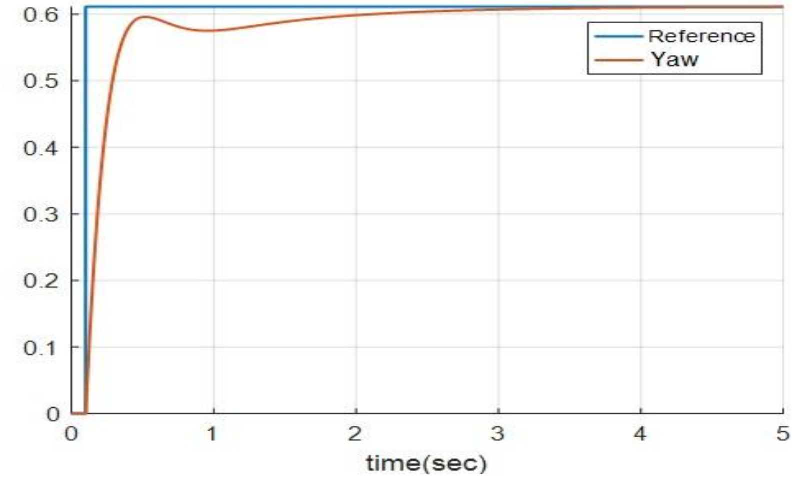

Figure 6: Closed loop simulation response of USV Yaw.

The simulation result for yaw rate response is shown in Figure 7. The yaw rate decays to zero within 1.5 seconds.

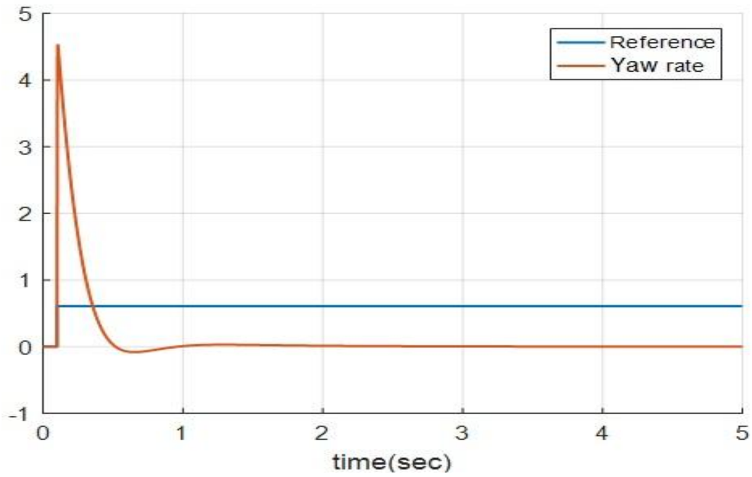

Figure 7: Closed loop simulation response of USV Yaw Rate.

The simulation result for manipulated variable response is shown in Figure 8. The magnitude of variable is within practical limits and drives the plant output to the desired reference signal.

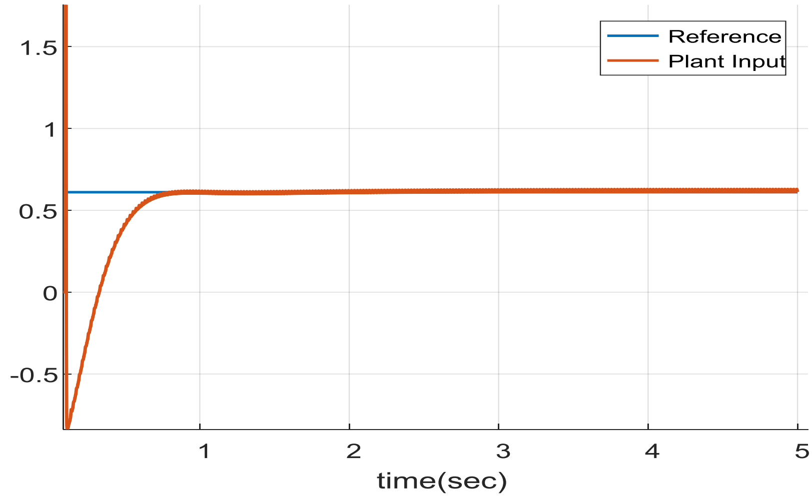

Figure 8: Closed loop simulation response manipulated variable.

The schematic representation of experimental hardware setup is shown in Figure 9.

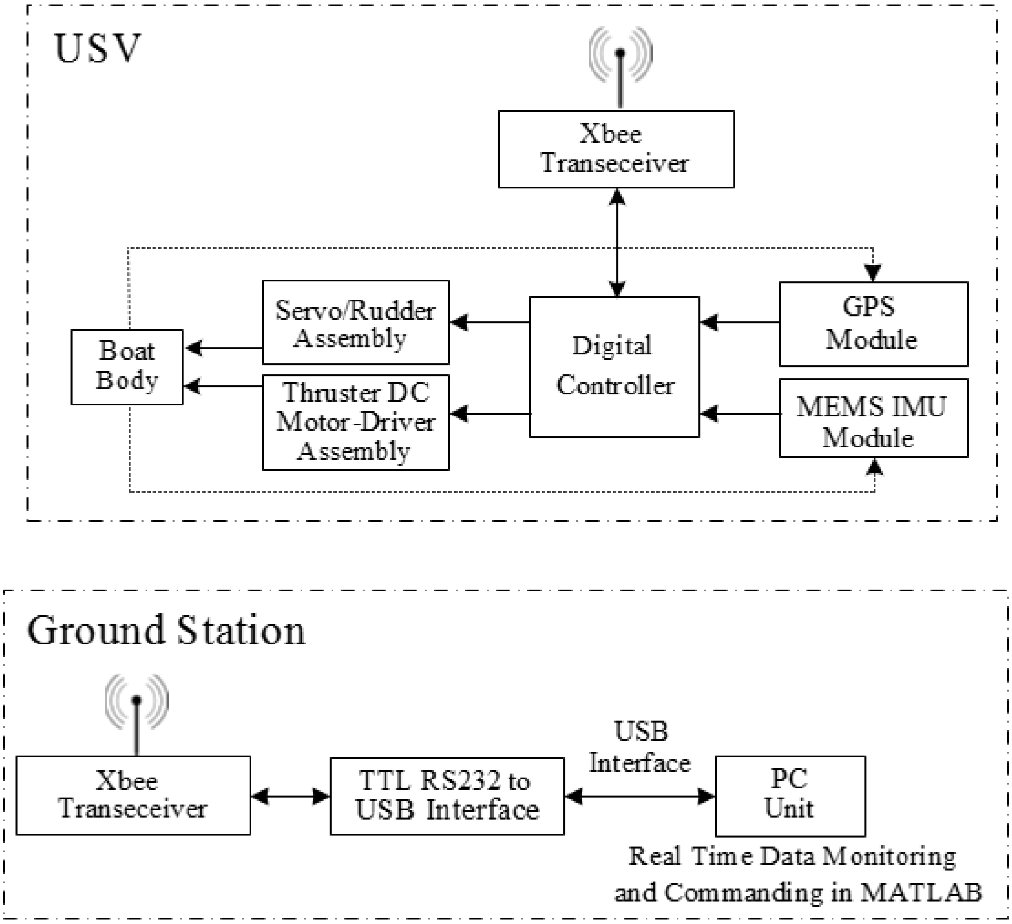

Figure 9: Schematic representation of hardware setup.

The experimental RCP Simulink model of the closed loop system with reference tracker is shown in Figure 10.

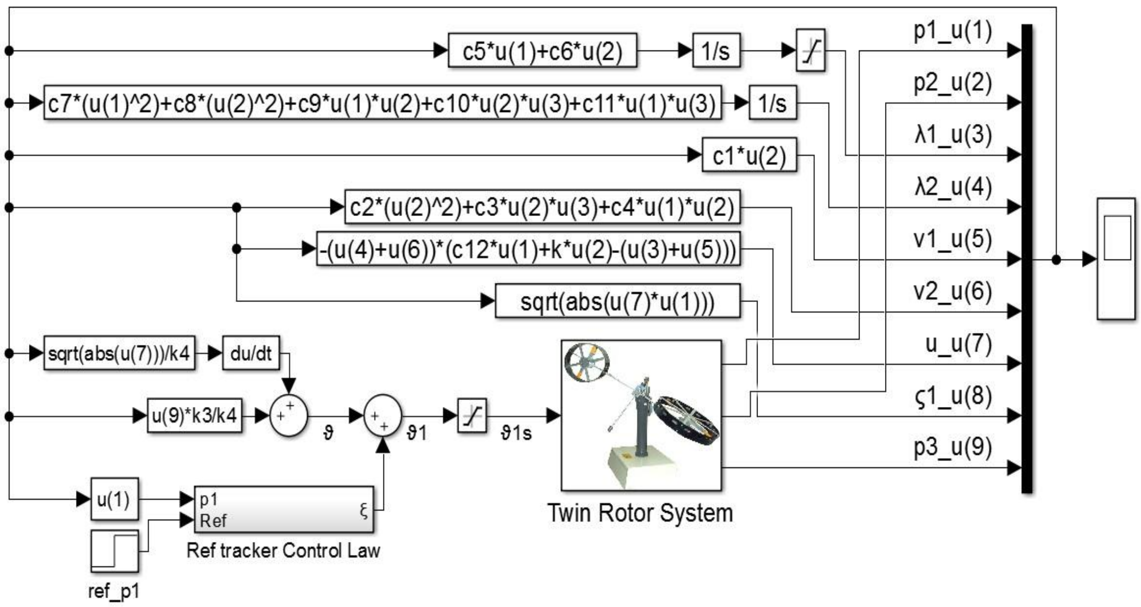

Figure 10: RCP mode of operation of testbed

The experimental result for yaw response is shown in Figure 11. The response is stable with zero steady state error.

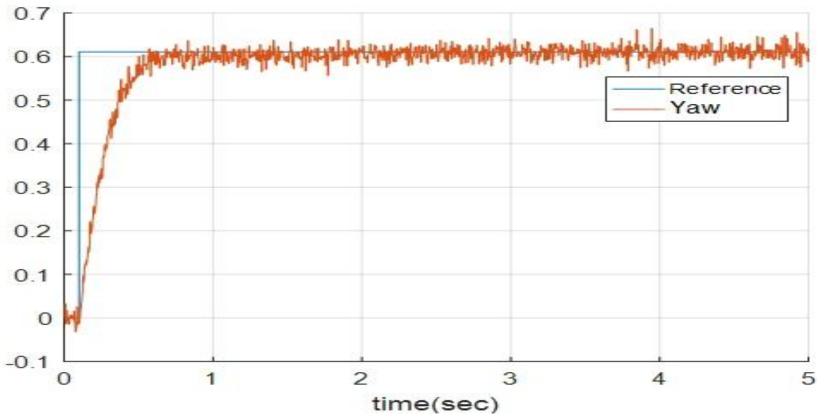

Figure 11: Experimental closed loop response of USV Yaw.

The experimental result for yaw rate response is shown in Figure 12. The yaw rate decays to zero within 1.5 seconds.

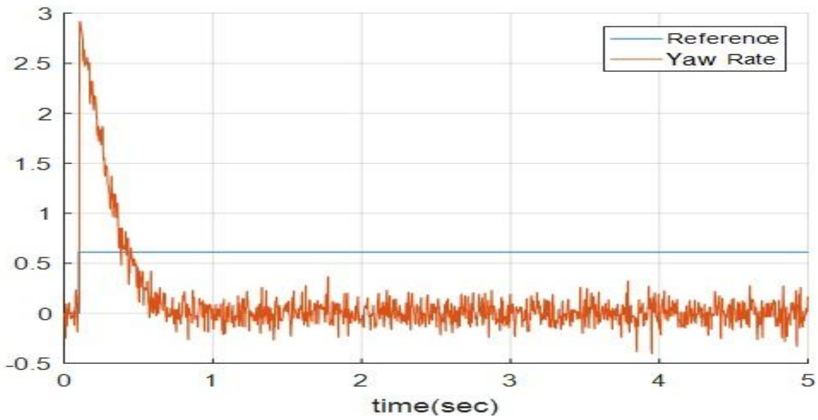

Figure 12: Experimental closed loop response of USV Yaw rate.

The experimental result for manipulated variable response is shown in Figure 13. The magnitude of variable is within practical limits and drives the plant output to the desired reference signal.

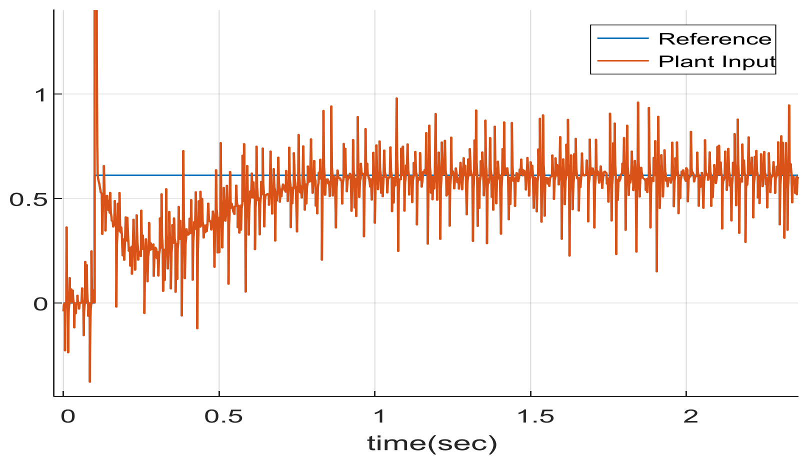

Figure 13: Experimental closed loop response of manipulated variable.

6. Conclusions

A robust nonlinear adaptive controller for the yaw dynamics or steering of a mini USV has been presented. System parameters are considered unknown and they are estimated using nonlinear adaptation. The proposed control technique is simulating in Simulink. The theoretical technique is tested in real time using digital controllers and data acquisition cards. The control algorithm has a lot of free tunable parameters. The results showed promising behavior of closed loop system in the presence of parameters uncertainties. Moreover, a greater control of closed loop system dynamics is possible owing to the flexibility in control algorithm.

References

[1] W. Li, Y. Li and X. Feng, "Study of the control system for an unmanned surface vehicle," 2013 IEEE International Conference on Signal Processing, Communication and Computing, KunMing, pp. 1-4, 2013.

[2] Y. Gao, N. Wang, S. Lv and M. J. Er, "Finite-time trajectory tracking control of unmanned surface vehicle with input saturation," IEEE International Conference on Underwater System Technology: Theory and Applications (USYS), Penang, Malaysia, pp. 150-154, 2016.

[3] L. Zhixiang, Z. Youmin, Y. Chi and L. Jun, "An adaptive linear parameter varying fault tolerant control scheme for unmanned surface vehicle steering control," 34th Chinese Control Conference (CCC), Hangzhou, pp. 6197-6202, 2015.

[4] L. Liu, D. Wang and Z. Peng, "Output feedback adaptive control for autopilot design of an unmanned surface vehicle," 5th International Conference on Information Science and Technology (ICIST), Changsha, pp. 419-423, 2015.

[5] H. Qu and K. D. von Ellenrieder, "Adaptive wind feedforward control of an Unmanned Surface Vehicle for station keeping," MTS/IEEE Washington, Washington, DC, pp. 1-10, 2015.

[6] Ke Feng, N. Wang, Dan Liu and M. J. Er, "Adaptive fuzzy trajectory tracking control of unmanned surface vehicles with unknown dynamics," 3rd International Conference on Informative and Cybernetics for Computational Social Systems (ICCSS), Jinzhou, pp. 342-347, 2016.

[7] M. Kumru, K. Leblebicioğlu, İ. K. Erünsal and K. Ahiska, "A survey on tactical control algorithms for path tracking unmanned surface vehicles," 14th International Conference on Control, Automation, Robotics and Vision (ICARCV), Phuket, pp. 1-6, 2016.

[8] S. Lv, N. Wang, Y. Gao and M. J. Er, "Disturbance observer based finite-time trajectory tracking control of unmanned surface vehicles," IEEE International Conference on Underwater System Technology: Theory and Applications (USYS), Penang, Malaysia, pp. 32-36, 2016.

[9] W. B. Klinger, I. R. Bertaska, K. D. von Ellenrieder and M. R. Dhanak, "Control of an Unmanned Surface Vehicle with Uncertain Displacement and Drag," IEEE Journal of Oceanic Engineering, 42(2), pp. 458-476, 2017.

[10] S.Qiaomei, R.Guang, Y.Jin and Q.Xiaowei, "SVM inverse model-based heading control of unmanned surface vehicle," IEEE Youth Conference on Information, Computing and Telecommunications, Beijing, pp. 138-141, 2010.

[11] A. Astolfi, andR. Ortega, "Immersion and invariance: a new tool for stabilization and adaptive control of nonlinear systems," IEEE Transactions on Automatic Control, 48(4), pp. 590–606, 2003.